



Chemistry & Biology Interface

An official Journal of ISCB, Journal homepage; www.cbijournal.com

Research Paper

Reaction Kinetics of Nucleophilic Substitution in the Synthesis of Moxifloxacin

Prashanth Reddy.G^{1,2}, Pemula Keerthi¹, Nagaraju Gudimalla¹, Sandeep Mohanty¹, Rakeshwar Bandichhor^{1*}

¹ API R&D, Integrated Product Development, Innovation Plaza, Dr. Reddy's Laboratories Ltd, Bachupally, Qutubullapur, Hyderabad-500072, A.P., India

² Center for Environment, Institute of Science and Technology, Jawaharlal Nehru Technological University, Kukatpally, Hyderabad 500072, A.P., India

Received 15 June 2012; Accepted 16 July 2012

Keywords: Demethylation, Moxifloxacin, Dynochem software, Reaction kinetics, nucleophilic substitution, alkyl ammonium salt

Abstract: Identification of reaction pathway during the synthesis of Moxifloxacin by using Dynochem software and the process optimization considering the reaction kinetics are described.

Introduction

Moxifloxacin hydrochloride (Avalox) **1** is a broad-spectrum antibacterial fluoroquinolone particularly effective against gram positive bacteria. Several processes based on the substitution have been developed for the preparation of Moxifloxacin **1**. Notably, direct and chelation controlled nucleophilic substitutions involving (*S,S*)-2,8-diazabicyclo(4,3,0) nonane **6** and 1-cyclopropyl-6,7-difluoro-8-methoxy-4-oxo-1,4-dihydroquinoline-3-carboxylic acid **4** were found to be well explored as shown in Scheme 1.^[1,2,4]

throughput of the direct nucleophilic substitution by involving **4** and **6**. Experiments conducted as per the reported literature^[1] afforded **1** in ~65% yields along with the impurities **2** & **3** as shown in Scheme 2. Purification of these impurities has not only increased the raw material cost but also generated huge amount of hazardous waste.

However the pathway of impurities formation is not well understood. First impurity **2** & **3** were synthesized and characterized, after that Dynochem software were used to determine the possible mechanism of formation of all the components during the reaction.

In our endeavor, we focused on improving

Results and Discussion

We attempted to develop relatively better process that can avoid the formation of

Corresponding Author* Tel.: +91 4044346117; fax: +91 40446285; e-mail: rakeshwarb@drreddys.com
#DRL-IPD Communication number: IPDO-IPM-00302

impurities during the synthesis. It was imperative to understand the precise reaction kinetics therefore we opted for Dynochem software as a tool. Dynochem is a modeling software originally developed at Zeneca in the mid-1990s by Frans Muller under the leadership of Keith Carpenter which exploits the curve fitting techniques and numerical methods to predict pathway and kinetic parameters of non elementary reactions.

There were two factors; concentration and time for all the components of the reaction. Subsequently, most probable reaction pathway has been taken into account for simulation. As expected, this software allowed us to understand the correlation of the predicted curves to fit in the experimental data. The degree of alignment of experimental data to the simulated curves validates the assumed reaction pathway.

Software, in this case, processes the data considering the most suitable pathway considering the stoichiometric order and rate equations of these elementary reactions in predicting the curve shape and therefore does not give an overall rate law. As a result, rate laws considering the stoichiometric order of reaction could be taken for each elementary reaction.

In the beginning, the starting material is sparingly soluble in acetonitrile, as reaction progresses the suspension attains clear solution. Therefore, the precise concentration can't be calculated. However, considering the area under the curve in HPLC can indicate the percentage quantity of starting material, product as well as by-product, these were further calculated in mmols which are featured in [Table 1]. The prerequisite data required were generated by conducting the experiments featured in [Table 1] which are not from single run instead there were seven individual reactions

performed to avoid sampling error. The data is presented in [Table 1] and Graphs 1 & 2.

Literature^[3] reports suggest that demethylation of **4** is due to the alkyl ammonium salt of hydrogen fluoride formed in the reaction. In order to understand and cross verify these events, we collected the data points as shown in Graphs 1&2. The model given to Dynochem as per Scheme 2 resulted in simulation curves as shown in the Graphs 3 & 4. We could clearly notice the deviation of simulated curves from the actual experimental data points. This indicates that the components follow a different mechanistic pathway as opposed to the path given in Scheme 2.

According the correlation studies as shown in Graphs 3&4 where the deviation of experimental data to the simulated curves was found to be quite significant, we concluded that the impurities formation can't be the function of full fledged HF which forms and gets stabilized in the form of alkyl ammonium salt.

We also observed that the impurities formation started in the beginning of the reaction parallel to the product formation; therefore we started investigating the fate of the reaction intermediates. Thus, we selected another model (2) and studied the curve fitting phenomenon as given below:

The kinetic parameters show that the rate of formation of product is faster compared to impurities **2** & **3**, therefore at any given time we see more quantity of product and the least quantity of the impurities **2** & **3**.

Mechanistically, in accordance with the software output, we can assume that the substrate **4** can react with the base to afford impurity **2** while intermediate **5** can afford the formation of product **1** along with the impurity

3. Transient fluoride can afford impurity **3** as shown in [Figure 1]. The formation of these two impurities may depend on the mild base that can take enolic proton in reaction intermediate **5** to maximize the product and minimize the impurities.

Having understood the reaction path way of nucleophilic substitution reaction, where the formation of product and the impurities are in parallel due to the reaction of base with the substrate **4** and intermediate **5**, we switch to screen the bases.

We decided to screen different bases, before we embarked our studies on substitution reaction we realized that it is important to investigate the impact of base on the starting material **4** that presumably can afford impurity **2**. The screening results are summarized in [Table 2]. This exercise indicated that only ~1% [entry 6] of impurity **2** was formed in presence of diisopropylethylamine (DIPEA) while ~97% [entry 15] of **2** was formed in presence of tetramethyl-1,6-hexadamine. We attempted demethylation of **4** by using NMP (polar solvent) in combination with pyridine or triethyl amine, tetramethylethylene diamine. In all the cases we observed demethylation at a faster rate than acetonitrile.

Base screening results on **4** suggested that DIPEA (sterically hindered base) can afford the product **1** with minimum percentage of impurities.

Thus we used DIPEA instead of triethyl amine (that was originally used in the precedented approach) in the nucleophilic substitution reaction that provided improved results. The conversion of the product increased from 77.5 to 88.89% and the impurities were significantly reduced as shown in [Table 3] [entry 2]. The reaction

termination was based on almost disappearance of **4**.

Reaction tolerance with respect to different solvents e.g. NMP, DMSO, DMF and DMA was tested. As mentioned in [Table 4], none of them has afforded better results than acetonitrile.

Conclusion

Considering the outcome of the reaction kinetics with the help of Dynochem software, we were able to identify the possible reaction pathway and the role of suitable base in order to obtain improved yield with significantly reduced levels of impurities. This advancement enabled us to stream line the process during the manufacturing of the Moxifloxacin **1** with impressive isolated yield (>80%) and purity (>99.9%).

Experimental Section

General: Starting material (S,S)-2,8-diazabicyclo(4,3,0)nonane **6** and 4-(1-cyclopropyl-6,7-difluoro-8-methoxy-4-oxo-1,4-dihydroquinoline-3-carboxylic acid) **4** were taken from commercial available source, and other reagents were used as such without further purification. HPLC and Chiral HPLC were performed with Waters' instrument using ACE C18, 250X 4.0 mm ID, 5 μ particle size or equivalent. The FT-IR spectra were recorded in the solid state KBr/Neat dispersion using Shimadzu IR Prestige-21 spectrophotometer. The ^1H and ^{13}C NMR spectra were recorded in DMSO- d_6 /CDCl $_3$ on Varian 500 & 400 MHz; the chemical shifts were reported in δ ppm relative to TMS. The melting points were determined by using the capillary method on POLMON (ModelMP96) melting point

apparatus. Dynochem software was provided by India soft Technologies (P) Ltd.

1-Cyclopropyl-7[S,S]-2,8-diazabicyclo[4,3,0]non-8-yl)-6-fluoro,1,4-dihydro-8-methoxy-4-oxo-3-quinoline carboxylic acid hydrochloride 1

To a solution of 50 g (0.169 mol) of 1-cyclopropyl-6, 7-difluoro-1, 4-dihydro-8-methoxy-4-oxo-3-quinolinecarboxylic acid **4** in acetonitrile (250 mL) DIEPA (0.213 mol; 27.5 g) was added under stirring (10-15 min.) at room temperature. Thereafter, (S,S)-2,8-diazabicyclo(4,3,0) nonane **6** (0.204 mol; 25.5 g) was added to the solution at 25 °C. The reaction mass was heated to reflux (78°C) for 15 h, after completion of the reaction, reaction mass was cooled to room temperature and pH of the reaction mass was adjusted to 5.5 to 6 with concentrated HCl. Precipitated material filtered and washed with 50 mL of acetonitrile.

Above wet material was added to 220 mL of 20% aq. methanol and continued stirring for 10 min. 25 °C. Subsequently, the pH of the reaction mass was adjusted to 8.5 to 9 with 12% aq. Ammonia and un-dissolved material was filtered. The pH of the filtrate was adjusted <2 with concentrated HCl and continued the stirring for 30 min. at 10 °C. The precipitated material was filtered and washed with 20 mL of chilled methanol.

Above wet material was suspended into 180 mL of aq. methanol at room temperature and heated to reflux for 1 h, followed by cooling it to 10°C and filtered the material and washed with 20 mL of methanol. The above material was subjected to reflux for 6 to 8 h in MIBK (8 vol.) to remove water azeotropically that afforded anhydrous Moxifloxacin hydrochloride **1**; Yield 59.5 g, (80.24%); purity by HPLC 99.91%; Chiral purity: 99.95%; mp: 246-248 °C; IR (KBr)

3363 cm⁻¹ (OH/NH), 2933cm⁻¹ (aliphatic CH), 1731 cm⁻¹ (C=O), 1515 cm⁻¹ (aromatic C=C), 1455 cm⁻¹ (aliphatic CH), 1185 cm⁻¹ (C-O-C, aryl alkyl ether), 1160 cm⁻¹(C-F), 1105 cm⁻¹ (C-N), 803 cm⁻¹ (aromatic CH); ¹HNMR (400 MHz, DMSO-d₆) δ 15.13 (br, s, 1H), 10.11 (br, s,1H), 8.88 (br, s, 1H), 8.66 (s, 1H), 7.65 (d, 1H, J=14.0 Hz), 4.12 – 4.17 (m,1H), 4.05 (dd, 1H, J=5.6 Hz, J=5.2Hz), 3.85 – 3.89 (m, 1H), 3.72 – 3.77 (m, 2H), 3.59 (s, 3H), 3.16 (d, 1H, J=12.8Hz), 2.89 (t, 1H, J=9.2Hz), 2.65 – 2.66 (m, 1H), 1.68 – 1.83 (m, 4H), 1.19 – 1.23 (m, 1H), 1.10 – 1.17 (m, 1H), 0.90 – 1.09 (m, 1H), 0.85 – 0.89 (m, 1H); ¹³C NMR (400 MHz, DMSO-d₆) δ 175.94, 165.81, 153.67, 150.33, 140.34, 136.67, 134.49, 117.28, 106.63, 106.38, 61.83, 54.44, 54.05, 51.87, 41.44, 40.59, 34.10, 20.48, 17.50, 9.56, 8.34; Calculated (M⁺) for C₂₁H₂₄FN₃O₄: 401.2; found (MH⁺) 402 (MH⁺).

1-cyclopropyl-6-fluoro-7-((4aS,7aS)-hexahydro-1H-pyrrolo[3,4-b]pyridin-6(2H)-yl)-8-hydroxy-4-oxo-1,4-dihydroquinoline-3-carboxylic acid (3)

10 g, (0.022 mol, 1.0 eq) of 1-cyclopropyl-6-fluoro-7-((4aS,7aS)-hexahydro-1H-pyrrolo[3,4-b]pyridin-6(2H)-yl)-8-methoxy-4-oxo-1,4-dihydroquinoline-3-carboxylic acid hydrochloride **1** was added to 30 mL of NMP, 7 g, (0.027 mol, 2.0 eq) of HI was added with stirring at room temperature and warmed the reaction mass to 130 °C for 5 h, after completion of the reaction, concentrated under reduced pressure at below 100 ° C, cooled to 60°C,100 mL of water was added and pH of the reaction mass was adjusted to 7.5 – 8.0 with ~7 mL, of caustic soda lye solution with stirring at room temperature, compound was extracted with 2 X 250 mL of DCM, combined organic layer was dried over Na₂SO₄, final organic layer was concentrated under

reduced pressure at below 45 °C, 50 mL of acetone was added with stirring, cooled the reaction mass to 10°C for 30 – 45 minutes, filtered the precipitated material and dried at room temperature to furnish 6 g, (0.015 mol, 67%) of 1-cyclopropyl-6-fluoro-7-((4*aS*,7*aS*)-hexahydro-1*H*-pyrrolo[3,4-*b*]pyridin-6(2*H*)-yl)-8-hydroxy-4-oxo-1,4-dihydroquinoline-3-carboxylic acid (3). IR (KBr) 3451 cm⁻¹ (OH/NH), 3103 cm⁻¹ (aromatic CH), 2926 cm⁻¹ (aliphatic CH), 1728 cm⁻¹ (C=O), 1606 cm⁻¹ (aromatic C=C), 1456 cm⁻¹ (aliphatic CH), 1270 cm⁻¹ (C-N), 1189 cm⁻¹ (C-F), 1038 cm⁻¹ (C-O), 804 cm⁻¹ (aromatic CH); ¹H NMR (400 MHz, CDCl₃) δ 8.74 (s, 1H), 7.46 (d, 1H, J=9.6Hz), 4.34- 4.36 (m, 1H), 3.67 (dd, 1H, J=2.4 Hz, J=3.2Hz), 3.49 (t, 1H, J=9.6 Hz), 3.22 -3.28 (m, 3H), 2.89 (d, 1H, J=11.2), 2.81 (t, 2H, J=12), 1.67 – 1.88 (m, 4H), 1.08 – 1.25 (m, 4H); ¹³C NMR (400 MHz, DMSO-*d*₆) δ 176.23, 165.62, 158.6, 149.42, 146.61, 129.65, 129.16, 123.25, 105.96, 101.54, 55.99, 55.19, 51.48, 42.02, 41.74, 34.70, 20.72, 16.60, 9.42, 9.08; Calculated (M⁺) for C₂₀H₂₂FN₃O₄: 387.3; found (MH⁺) 388.2.

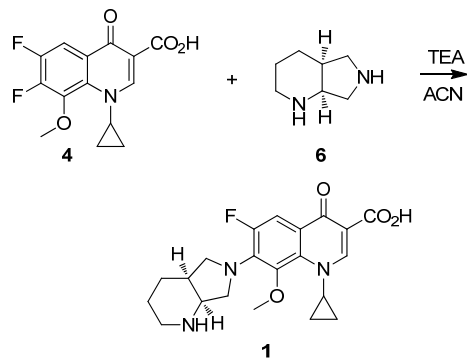
1-cyclopropyl-6,7-difluoro-8-hydroxy-4-oxo-1,4-dihydroquinoline-3-carboxylic acid (2)

8.2 g. (0.20 mol, 3.0 eq) of caustic soda flakes was dissolved in 100 mL of water with stirring at room temperature, 20 g, (0.068 mol, 1.0 eq) of 1-cyclopropyl-6,7-difluoro-8-methoxy-4-oxo-1,4-

dihydroquinoline-3-carboxylic acid (4) was added and warmed the reaction mass to 100 ° C for 10 h, after completion of the reaction, cooled to 80 °C and treated with 2 g of activated charcoal at 80°C, and filtered through hyflow and washed with 40 mL of water, pH of the combined filtrate were adjusted to 4 – 5 with ~8 mL of acetic acid at 40°C, cooled the reaction mass to room temperature for 30 – 60 minutes, filtered the precipitated material and washed with 20 ml of water and dried the material at 100 °C to furnish the 17 g, (0.06 mol, 89%) of 1-cyclopropyl-6,7-difluoro-8-hydroxy-4-oxo-1,4-dihydroquinoline-3-carboxylic acid (2). IR (KBr) 3458 cm⁻¹ (OH), 3065 cm⁻¹ (aromatic CH), 1732 cm⁻¹ (C=O), 1622 cm⁻¹ (aromatic C=C), 1466 cm⁻¹ (aliphatic CH), 1188 cm⁻¹ (C-F), 1039 cm⁻¹ (C-O), 804 cm⁻¹ (aromatic CH); ¹H NMR (500 MHz, DMSO-*d*₆) δ 14.76 (s, 1H), 11.67(s, 1H), 8.70 (s,1H), 7.67 (t, 1H, J=10 Hz), 4.30 – 4.35 (m, 1H), 1.13 – 1.15 (m, 4H); ¹³C NMR (500 MHz, DMSO-*d*₆) δ 176.37, 165.49, 150.27, 149.88, 145.01, 142.93, 139.53, 130.17, 122.97, 106.44, 101.91, 41.67, 9.36. Calculated (M⁺) for C₁₃H₉F₂NO₄: 281.05; found (M⁻) 280.0.

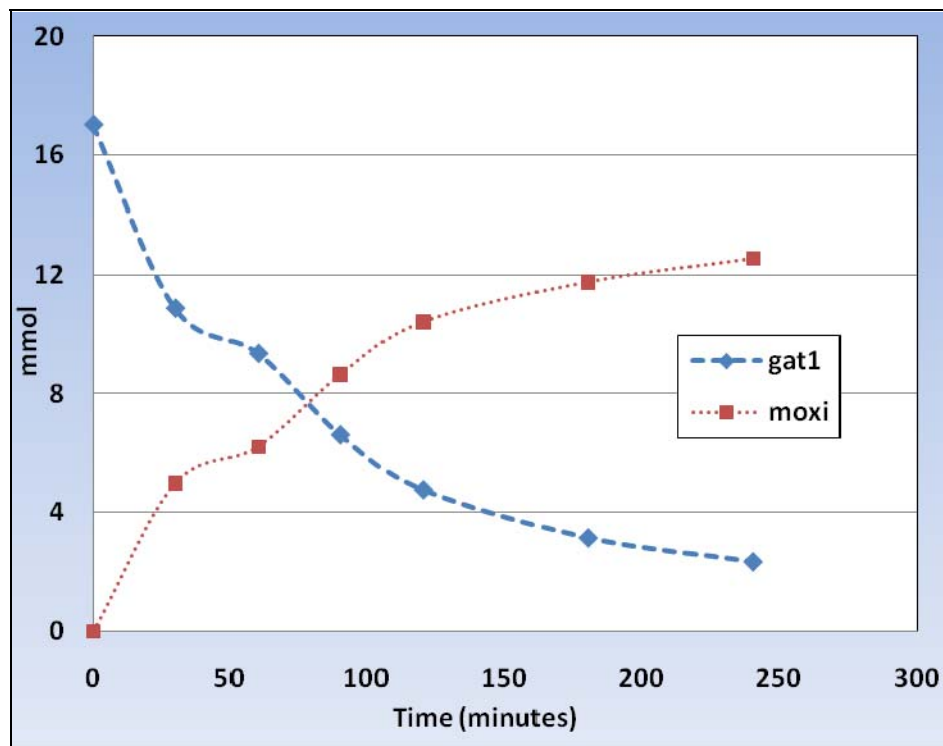
Acknowledgment

We thank the management of R&D-CTO & IPDO, Dr. ReddysLaboratories Ltd., for supporting this work. Cooperation from analytical research development colleagues is highly appreciated.

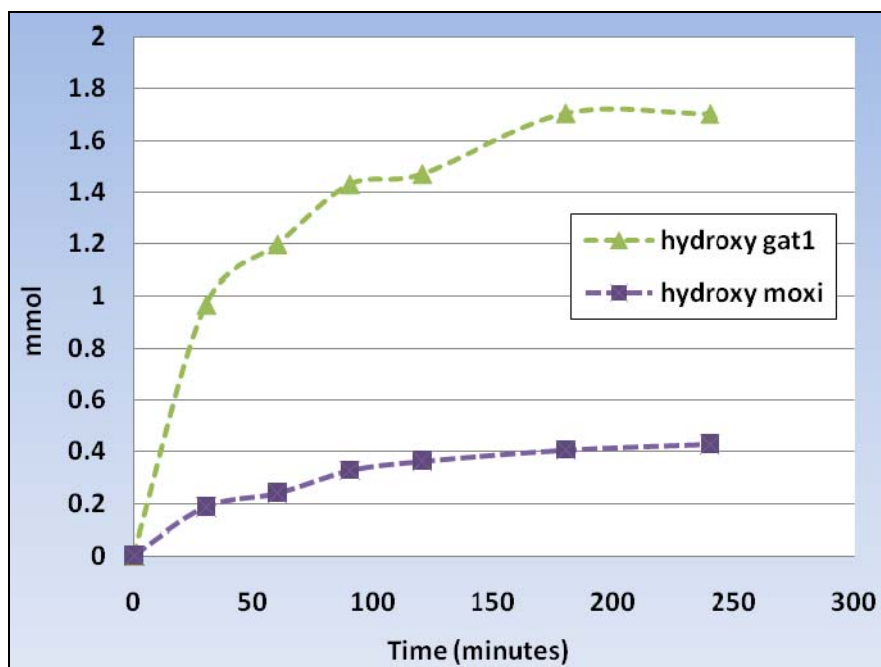
**Scheme-1: Precedented scheme for Moxifloxacin (1)****Table 1.** Data points of nucleophilic substitution of **6** on **4** at different time intervals

S.No.	Time (h)	1 (mmol)	4 (mmol)	2 (mmol)	3 (mmol)
1	0 min	0	16.94	0	0
2	30 min	4.98	10.87	0.97	0.19
3	60 min	6.22	9.34	1.2	0.24
4	90 min	8.64	6.6	1.43	0.33
5	120 min	10.42	4.75	1.47	0.36
6	180 min	11.77	3.13	1.7	0.41
7	240 min	12.55	2.32	1.7	0.43

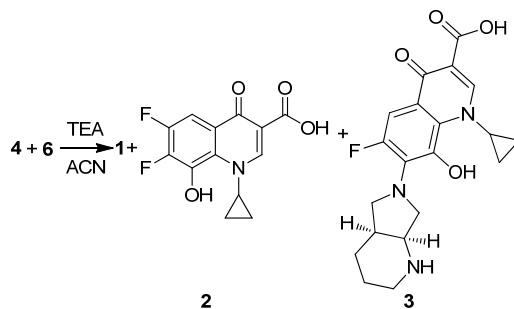
1.



2.



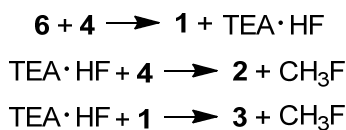
Graphs 1 & 2. Graphical representation of data points pertaining to [Table 1] (gat-1: 4; moxi: 1; hydroxy gat-1: 2 and hydroxy moxi: 3)



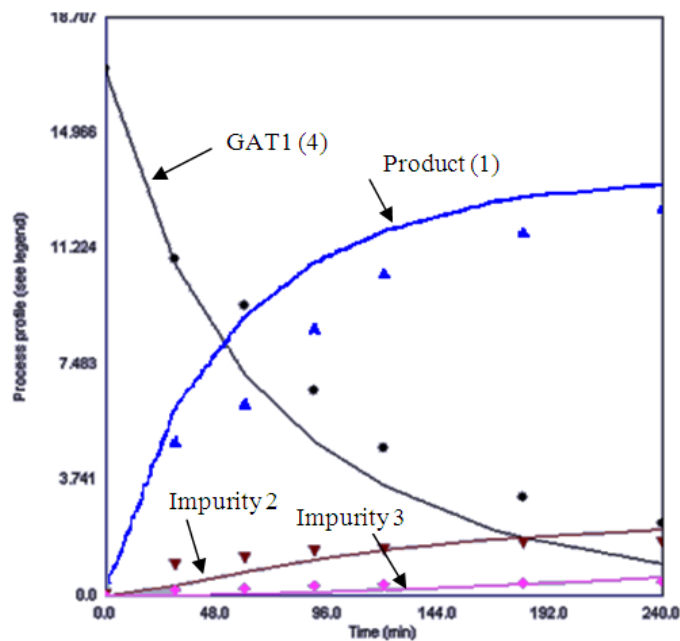
Scheme 2. Precedented approach for impurities formation based on the literature

According to Scheme 2, the equation and graphs by employing Dynochem Model can be depicted as given below:

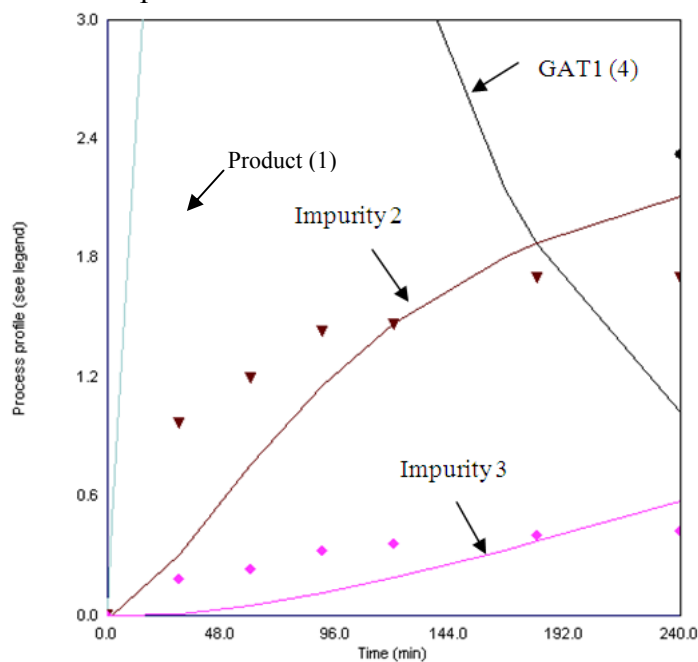
Model 1



3.

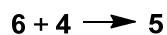


4. Expanded version of 3 for impurities 2 & 3

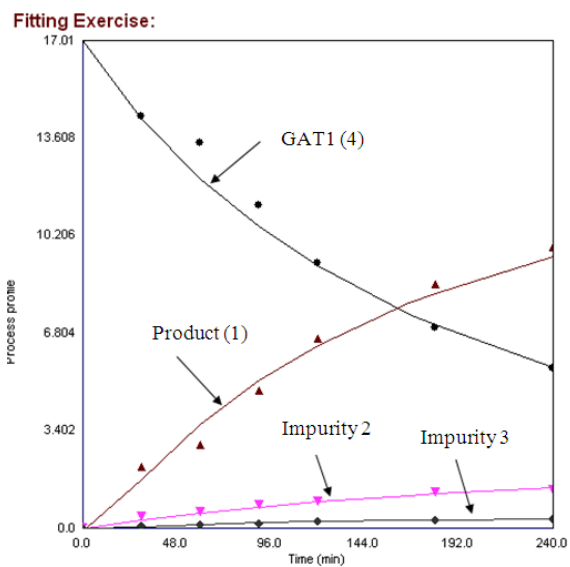


Graph 3 & 4: Correlation of data points: (The line represents the predicted features by Dynochem software considering the HF mediated demethylation and the points refers to the actual data generated from experiments)

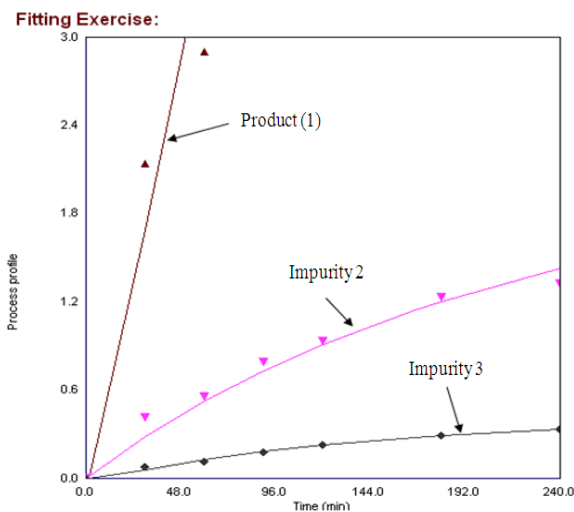
Model 2



5.



6.



The kinetic parameters obtained from the Dynochem simulation for Model 2.

$$k_1 = 1.5\text{E-}04 \text{ L/mol/sec at } 75^\circ\text{C}$$

$$k_2 = 1.2\text{E-}05 \text{ L/mol/sec at } 75^\circ\text{C}$$

$$k_3 = 1.7\text{E-}03 \text{ L/mol/sec at } 75^\circ\text{C}$$

$$k_4 = 7.2\text{E-}05 \text{ L/mol/sec at } 75^\circ\text{C}$$

L in rate law

Liter/mol/sec is the unit of rate constant according to stoichiometric orders.

$$r = k [A] [B]$$

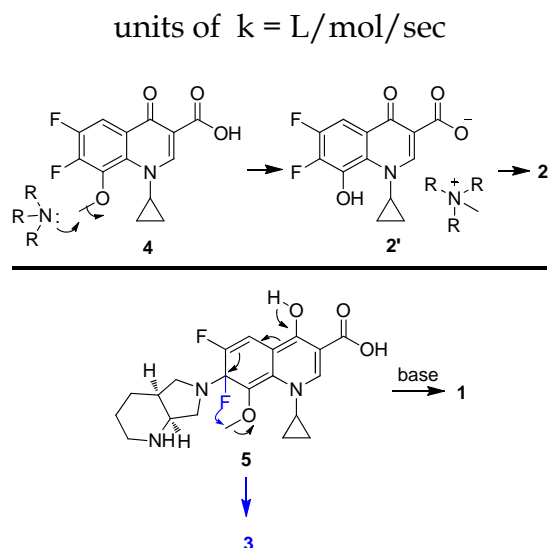


Figure 1. Proposed mechanism for product **1** as well as impurities **2** & **3** formation

Table 2. Demethylation of **4** by using different bases in acetonitrile* & NMP*

Entry	Base (2 eq)	Time (h)	NMP		Acetonitrile	
			2 (%)	4 (%)	2 (%)	4 (%)
1	Pyridine	10	4.5	83.08	1.33	98.21
2	Pyridine	20	7.04	79.36	3.78	94.87
3	Pyridine	30	9.75	74.16	5.8	92.13
4	DIPEA	10	0.91	92.05	0.426	98.886
5	DIPEA	20	1.28	91.3	0.343	99.2
6	DIPEA	30	2.56	89.55	1.06	97.81
7	TEA	10	27.37	68.44	21.8	76.29
8	TEA	20	37.24	56.91	30.81	66.47
9	TEA	30	43.99	48.83	39.41	57.18
10	TetramethylEDA	10	90	5.4	78.44	18.92
11	TetramethylEDA	20	94.94	0.77	91.57	5.35
12	TetramethylEDA	30	95.08	0.16	93.311	3.12
13	Tetramethyl-1,6-hexadiazine	10	94.95	1.67	92.3	5.18
14	Tetramethyl-1,6-hexadiazine	20	95.49	0.16	96.7	0.591
15	Tetramethyl-1,6-hexadiazine	30	95.07	0.07	96.89	0.05

*reaction temperature: 78 °C

Table 3: Reaction of **4** with **6** by using different bases in 5 volumes of acetonitrile

Entry	1.25 eq. Base	Temp. (°C)	Nonane (eq)	Time (h)	1 (%)	1* (%)	2 (%)	3 (%)	4 (%)
1	Pyridine	78	1.2	15	82.56	74.2	6.27	2.47	0.24
2	DIPEA	78	1.2	15	88.89	80.45	4.2	0.8	0.46
3	TEA	78	1.2	10	77.5	68	7.83	2.23	0.42
4	TetramethylEDA	78	1.2	10	73.5	58.6	10.65	1.55	0.045
5	Tetramethyl-1,6-hexadiazine	78	1.2	10	71.5	59	10.69	1.67	0.06

*isolated yield

Table 4: Reaction of **4** with **6** by using DIEPA as a base in different solvents

Entry	Solvent	Temp. (°C)	Nonane (eq)	Time (h)	1 (%)	1* (%)	2 (%)	3 (%)	4 (%)
1	NMP	78	1.2	10	84.7	76.2	4.8	2.23	0.78
2	DMSO	78	1.2	10	84.47	77.2	5.5	2.91	0.71
3	DMF	78	1.2	10	82.27	74.5	5.9	2.82	1.76
4	DMA	78	1.2	10	82.68	73.8	5.6	3.08	1.24

*isolated yield

References

- [1] a) Petersen, U.; Schenke, T.; Philipps, T.; Grohe, K.; Bremm, K.; Endermann, R.; Metzger, K.; Haller, I. EP0550903. b) Petersen, U.; Schenke, T.; Krebs, A.; Grohe, K.; Schriewer, M.; Haller, I.; Metzger, K.; Endermann, R.; Zeiler, H. EP0350733 c) Zerbes, R.; Naab, P.; Franckowiak, G.; Diehl, H. EP0657448 d) Petersen, U.; Schenke, T.; Andreas, K.; Klaus, G.; Michael, S.; Haller, I.; Metzger, K.; Endermann, R.; Hans-Joachim, Z. U.S. 4,990, 517. e) Gehring, R.; Mohrs, K.; Heilmann, W.; Diehl, H. WO99 26940. f) Rudolf, Z.; Paul, N.; Gerhard, F.; Herbert, D. U.S.5639886. f) Masuzawa, K.; Suzue, S.; Hirai, K.; Ishizaki, T.; EP230295
- [2] a) Japanese patent Kokai Sho 63-198664 (2) Falomo, Nicolau.; Villasante, Prieto.; Fernandez, L.; Molina P.; EP 1832587. b) Naomi Takagi, N.; Hironobu, F.; Hiroshi, M.; U.S. 5, 157, 117 (2) Satyanarayan, C.; Seetaramanjanyulu, G.; Umamaheswararao, V.; Lakshmi Narasimharao, D.V.; WO2005, 012285. c) Ramachandrarao, D.; Narayan rao, K.R.; Srinivas, P. L.; Ravikumar, P.; Manish, G.; Sheshirekha, K.; WO2008059223. d) Andrea castellan, M.; Pierluigi Padovan, C.; Liu Jiageng, H.; Yibo Zhou, H.; Lin Feng, H.; U.S.2011 0230661.
- [3] F. Javier, V.; Lourdes, G.; Sara, P. F.; Olga, A.; Elena, G.; Antonio, C. *Org. Process Res. Dev.* **2008**, *12*, 900–903.
- [4] Satyanaraya Reddy, B.; Venkat Reddy, Y.; P. V. Varaprasada Reddy, P. Indian Pat. Appl. IN 2012CH00223 A 20120127